Research Article Open Access

Shun-Cai Zhao*, Qi-Xuan Wu, and Kun Ma

2-D isotropic negative refractive index in a N-type four-level atomic system

DOI 10.1515/phys-2015-0043

Received May 23, 2015; accepted October 06, 2015

Abstract: 2-D(Two-dimensional) isotropic negative refractive index (NRI) is explicitly realized via the orthogonal signal and coupling standing-wave fields coupling the N-type four-level atomic system. Under some key parameters of the dense vapour media, the atomic system exhibits isotropic NRI with simultaneous negative permittivity and permeability (i.e. left-handedness) in the 2-D x-y plane. Compared with other 2-D NRI schemes, the coherent atomic vapour media in our scheme may be an ideal 2-D isotropic NRI candidate and has some potential advantages, significance or applications in the further investigation.

Keywords: 2-D; isotropic negative refractive index; left-handedness

PACS: 42.50.Gy; 32.80.Qk; 32.10.Dk; 78.20.Ci

1 Introduction

J.B. Pendry, *et al.* asserted that a medium with negative effective permeability can be achieved by the split-ring resonator (SRR) in free space [1], which has been studied to increase the permeability of artificial dielectrics in the 1952s [2]. Smith *et al.* combined the SRR with thin wires to design the NRI medium in 2000 [3]. And a year later, this SRR/wire composite medium was implemented and experimentally verified negative refraction for the first time [4]. The implementation has given rise to the NRI media because of its exotic properties. In particular, the possible sub-wavelength resolving properties [1] have stirred much excitement and renewed interest in electromagnetic phe-

With the development of investigating the NRI media, the requirement of 2-D NRI media is emerging. And several schemes [6–11] for 2-D NRI media have been proposed recently. However, most of the proposed 2-D NRI media are based on photonic crystal nanostructure or transmission line structure, and most of them are anisotropic, i.e., their exotic properties are polarization dependent, which is undesirable in certain potential applications, e.g., in "perfect lens" [1]. As an alternative, the arbitrary linear incident polarization via the printable NRI media have been proposed by C. Imhof *et al.* [12].

Here, we first explore the possibility of implementing 2-D NRI media by using the quantum coherence effect [13–16] in a four-level atomic system, which is driven by the orthogonal signal and coupling standing-wave fields. Thus, we can explicitly investigate the left-handedness and NRI of the resonant atomic system in the x-y plane. A few specific NRI values exhibit circular and homogeneous distributions in the x-y plane, and the atomic system possesses negative permittivity and permeability simultaneously.

2 Model and equation

Consider a N-type four-level atomic system with two lower states $|1\rangle$ and $|2\rangle$, two excited states $|3\rangle$ and $|4\rangle$, which interacts with three optical fields, i.e., the weak probe light Ω_p and two strong coherent coupling standing-wave fields $\Omega_c(x)$, $\Omega_s(y)$, respectively [see Figure 1]. Levels $|1\rangle$ and $|2\rangle$ have the same parity and level $|2\rangle$, $|3\rangle$ with an opposite parity. Thus the electric and magnetic components of the weak probe light field couple the electric-dipole transition $|3\rangle$ - $|2\rangle$ and the magnetic-dipole transition $|1\rangle$ - $|2\rangle$, respectively. Such anthe atomic system may be realized in $^{171}Yb(I=1/2)$. The states $|1\rangle$, $|2\rangle$, $|3\rangle$ and $|4\rangle$ correspond to $|^1S_0$, F=1/2, $m_F=1/2\rangle$, $|^1S_0$, F=1/2, $m_F=1/2\rangle$, $|^1P_1$, F=1/2, $m_F=1/2\rangle$ and $|^3P_1$, F=1/2, $m_F=1/2\rangle$, respectively.

The Rabi frequencies corresponding to the two orthogonal standing-wave fields are $\Omega_c(x) = d_{13}E_c/\hbar = \Omega_{c0}sin(k_1x), \Omega_s(y) = d_{14}E_c/\hbar = \Omega_{s0}sin(k_2y),$

Kun Ma: Physics department, Kunming University of Science and Technology, Kunming, 650500, PR China

nomena associated with NRI medium, first investigated by Veselago in the 1960s [5].

^{*}Corresponding Author: Shun-Cai Zhao: Physics department, Kunming University of Science and Technology, Kunming, 650500, PR China, E-mail: zscgroup@kmust.edu.cn

Qi-Xuan Wu: College English department, Kunming University of Science and Technology, Kunming, 650500, PR China

350 — S.-C. Zhao et al. DE GRUYTER OPEN

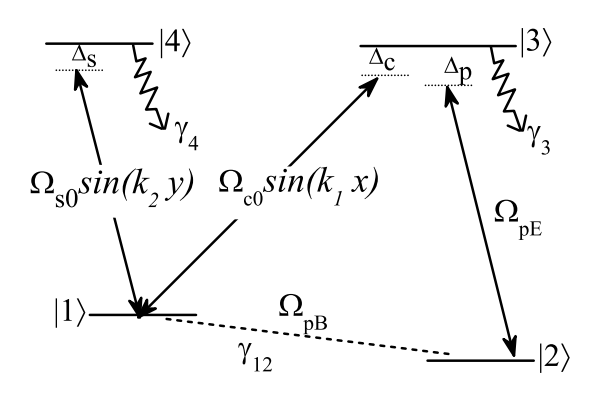


Figure 1: Schematic diagram of a four-level N-type atomic system. The electric-dipole transitions $|1\rangle - |4\rangle$ and $|1\rangle - |3\rangle$ are driven by two orthogonal standing-wave fields $\Omega_c(x)$ and $\Omega_s(y)$, respectively. The level pairs $|3\rangle - |2\rangle$ and $|1\rangle - |2\rangle$ are coupled to the electric and magnetic components of the weak probe light, respectively. $\gamma_{3,4}$ and γ_{12} denote the spontaneous decay rates and the dephasing rate, respectively.

respectively. E_c , E_s are the electric field strength envelopes of the two orthogonal standing-wave fields. k_i =2 π/λ_i , (i = 1, 2) is the wave vector with wavelengths λ_i , (i= 1, 2) of the corresponding standing wave fields. And the two orthogonal signal and coupling standing-wave fields drive the transitions $|1\rangle$ - $|4\rangle$ and $|1\rangle$ - $|3\rangle$, respectively. The frequency detunings of these three optical fields are Δ_p , Δ_c and Δ_s , respectively. At a low temperature, the atoms are assumed to be nearly stationary and hence any Doppler shift is neglected. Under the rotating-wave approximations the equations of motion for the probability amplitudes of the atomic system in the x-y plane are given as follows,

$$\begin{array}{rcl} \frac{\partial A_1(x,y)}{\partial t} & = & \frac{i}{2} \left(\Omega_{pE}^{\star} A_3(x,y) + \Omega_{pB}^{\star} A_2(x,y) \right) \\ \frac{\partial A_2(x,y)}{\partial t} & = & -i(\Delta_p - \Delta_c) A_2(x,y) + \frac{i}{2} (\Omega_c^{\star}(x) A_3(x,y) \\ & + & \Omega_s^{\star}(y) A_4(x,y)) + \frac{i}{2} \Omega_{pB}^{\star} A_1(x,y) \end{array} \tag{1}$$

$$\frac{\partial A_3(x,y)}{\partial t} & = & -i\Delta_p A_3(x,y) + \frac{i}{2} (\Omega_c(x) A_2(x,y) \\ & + & \Omega_p A_1(x,y)) - \frac{\Gamma_3}{2} A_3(x,y),$$

$$\frac{\partial A_4(x,y)}{\partial t} & = & -i (\Delta_p + \Delta_s - \Delta_c) A_4(x,y) + \frac{i}{2} \Omega_s(y)$$

$$A_2(x,y) - \frac{\Gamma_4}{2} A_4(x,y).$$

where the electric and magnetic Rabi frequencies of the probe light are defined by $\Omega_{pE} = d_{23}E_p/\hbar$, $\Omega_{pB} = \mu_{12}B_p/\hbar$, respectively. Here, E_p and B_p denote the electric and magnetic field strength envelopes of the probe light. The frequency detunings are defined by $\Delta_p = \omega_{32} - \omega_p$, $\Delta_c = \omega_{31} - \omega_c$,

and Δ_s = ω_{41} – ω_s . Where ω_p , ω_c and ω_s are the mode frequencies of the probe and two orthogonal standing-wave fields. $\Gamma_{3,4}$ and γ_{12} in Equation (1) denote the spontaneous decay rates and the dephasing rate, respectively.

When the intensity of the probe light is sufficiently weak and the temperature is very low, all the atoms remain in the ground state and the atomic population in level $|3\rangle$ is close to unity [17] without any Doppler shift. Under these conditions, the steady solutions of Equation (1) take the following forms

$$A_{2}(x,y) = \frac{1}{\xi(x,y)} \left[\frac{\gamma_{4}}{2} + i(\Delta_{s} + \Delta_{p} - \Delta_{c}) \right] \left[\frac{\Omega_{c}^{*}(x)\Omega_{pE}}{4} - \frac{i}{2} \cdot \left(\frac{\gamma_{3}}{2} + i\Delta_{p} \right) \Omega_{pB} \right],$$

$$A_{3}(x,y) = -\frac{i}{2\xi(x,y)} \left[\frac{\gamma_{4}}{2} + i(\Delta_{s} + \Delta_{p} - \Delta_{c}) \right]$$

$$\cdot \left\{ \left[\frac{\gamma_{12}}{2} + i(\Delta_{p} - \Delta_{c}) \right] \Omega_{pE} + \frac{i}{2} \Omega_{c}(x)\Omega_{pB} \right\}$$

$$- \frac{i}{8\xi(x,y)} \Omega_{s}(y)\Omega_{s}^{*}(y)\Omega_{pE}, \qquad (2)$$

$$A_{4}(x,y) = -\frac{i}{2\xi(x,y)} \left[-\frac{1}{4} \Omega_{pE} \Omega_{c}^{*}(x) + \frac{i}{2} \left(\frac{\gamma_{3}}{2} + i\Delta_{p} \right) \Omega_{pB} \right] \Omega_{s}(y),$$

with the parameter

$$\begin{split} \xi(x,y) &= -\left\{\frac{\Omega_c(x)\Omega_c^{\star}(x)}{4} + \left[\frac{\gamma_{12}}{2} + i(\Delta_p - \Delta_c)\right]\left(\frac{\gamma_3}{2} + i\Delta_p\right)\right\} \\ &\left[\frac{\gamma_4}{2} + i(\Delta_s + \Delta_p - \Delta_c)\right] - \frac{\Omega_s(y)\Omega_s^{\star}(y)}{4}\left(\frac{\gamma_3}{2} + i\Delta_p\right), \end{split}$$

In the following, we consider the electric and magnetic responses of the N-type four-level atomic system interacting with two orthogonal stand-wave light fields.

Considering the distinction between the applied fields and the microscopic local fields acting upon the atoms when discussing the detailed properties of the atomic transitions between the levels relating to the electric and magnetic susceptibilities, there is little difference between the macroscopic fields and the local fields [18, 21] in the dilute vapour case. However, the polarization of neighbouring atoms gives rise to an internal field at any given atom in addition to the average macroscopic field. In order to achieve the negative permittivity and permeability one should consider the local field effect in dense media with closely packed atoms.

We first obtain the atomic electric and magnetic polarizabilities, and then consider the local field correction to the electric and magnetic susceptibilities of the coherent vapour medium. Using the definitions of atomic microscopic electric and magnetic polarizabilities [18, 19], we can arrive at the following parameters

$$\gamma_{e}(x,y) = \frac{id_{23}^{2}}{\hbar\varepsilon_{0}} \frac{\frac{\Omega_{s}(y)\Omega_{s}^{*}(y)}{4} + \left[\frac{\gamma_{12}}{2} + i(\Delta_{p} - \Delta_{c}) + \frac{i}{2}\frac{\mu_{12}}{cd_{23}}\Omega_{c}(x)\right] \left[\frac{\gamma_{4}}{2} + i(\Delta_{s} + \Delta_{p} - \Delta_{c})\right]}{\left\{\frac{\Omega_{c}(x)\Omega_{c}^{*}(x)}{4} + \left[\frac{\gamma_{12}}{2} + i(\Delta_{p} - \Delta_{c})\right] \left(\frac{\gamma_{3}}{2} + i\Delta_{p}\right)\right\} \left[\frac{\gamma_{4}}{2} + i(\Delta_{s} + \Delta_{p} - \Delta_{c})\right] + \frac{\Omega_{s}(y)\Omega_{s}^{*}(y)}{4} \left(\frac{\gamma_{3}}{2} + i\Delta_{p}\right)}$$
(3)

$$\gamma_{m}(x,y) = \frac{-2\mu_{0}\mu_{12}^{2}}{\hbar} \frac{\left[\frac{\gamma_{4}}{2} + i(\Delta_{S} + \Delta_{p} - \Delta_{c})\right] \left[\frac{\Omega_{c}^{*}(x)}{4} \frac{cd_{23}}{\mu_{12}} - \frac{i}{2} \left(\frac{\gamma_{3}}{2} + i\Delta_{p}\right)\right]}{\left\{\frac{\Omega_{c}(x)}\Omega_{c}^{*}(x)}{4} + \left[\frac{\gamma_{12}}{2} + i(\Delta_{p} - \Delta_{c})\right] \left(\frac{\gamma_{3}}{2} + i\Delta_{p}\right)\right\} \left[\frac{\gamma_{4}}{2} + i(\Delta_{S} + \Delta_{p} - \Delta_{c})\right] + \frac{\Omega_{S}(y)\Omega_{S}^{*}(y)}{4} \left(\frac{\gamma_{3}}{2} + i\Delta_{p}\right)}$$

$$(4)$$

In the above calculations, $\gamma_e(x,y)=\frac{2d_{23}^2A_3(x,y)}{\hbar\varepsilon_0\Omega_{pE}}$, $\gamma_m(x,y)=\frac{2\mu_0\mu_{12}A_2(x,y)}{B_p}$ and the relation between the microscopic local electric and magnetic fields $E_p/B_p = c$ has been inserted.

We have obtained the microscopic physical quantities $\gamma_{e,m}(x,y)$. However, what we are interested in is the macroscopic physical quantities such as the electric permittivity and magnetic permeability. According to both the electric and magnetic Clausius-Mossotti relations [18, 19], we can arrive at the relative electric permittivity $\varepsilon_r(x, y)$ and magnetic permeability $\mu_r(x, y)$ as follows

$$\varepsilon_{r}(x,y) = \frac{1 + \frac{2}{3}N\gamma_{e}(x,y)}{1 - \frac{1}{3}N\gamma_{e}(x,y)},$$

$$\mu_{r}(x,y) = \frac{1 + \frac{2}{3}N\gamma_{m}(x,y)}{1 - \frac{1}{3}N\gamma_{m}(x,y)}.$$

where N denotes the atomic concentration.

Results and discussions

Here we will demonstrate the 2-D isotropic NRI can truly arise in the four-level coherent atomic vapour media interacting with two orthogonal standing-wave fields in the x-y plane. And the strong electric and magnetic responses can bring about simultaneously negative permittivity and permeability. For the sake of more closing to reality, several key parameters are adopted from the form investigation. The parameters for the atomic electric and magnetic polarizability are chosen as: the electric and magnetic transition dipole moments d_{23} =3 × 10⁻²⁹C · m and $\mu_{12} = 1.3 \times 10^{-22} \text{C} \cdot \text{m}^2 \text{s}^{-1}$ [16], respectively. The density of atom N was chosen to be 2×10^{23} m⁻³ [21]. And the other parameters are scaled by $\gamma = 10^8 s^{-1}$: $\Gamma_3 = 0.3 \gamma$, $\Gamma_4 = 0.1 \gamma$. Because the dephasing rate is in general two or three orders of magnitude less than the spontaneous decay rates in a low-temperature vapour [22], the dephasing rate γ_{12} is small and set to be $10^{-3}\gamma$.

Then the three-dimensional plots depict the real part of relative permittivity $Re\{\varepsilon_r\}$, permeability $Re\{\mu_r\}$ and refraction index $Re\{n\}$ of the atomic system dependent

the probe detuning Δ_P as a function of (x, y), which are shown in Figures 2, 3 and 4, respectively. As shown in Figure 2, the real part of relative permittivity $Re\{\varepsilon_r\}$ has the negative value in the x-v plane and the spike-like peak at the coordinate $\{0.75\lambda, 0.75\lambda\}$ in Figure 2(a), Figure 2(b), Figure 2(c), Figure 2(d), respectively. We also noted $Re\{\varepsilon_r\}$ remains the negative values with the decreasing peaks when the values of Δ_p are tuned to be 5.0 γ , 5.3 γ and 5.7 γ , in Figure 2(b), Figure 2(c), Figure 2(d), respectively.

Figure 3 shows the three-dimensional plots for the $Re\{\mu_r\}$. It can be seen from Figure 3 that $Re\{\mu_r\}$ has negative values under the same condition as Figure 2. As shown in Figure 3 from (a) to (d), the increasing peak values of $Re\{\mu_r\}$ are observed when Δ_p was tuned to be 4.7γ , 5.0γ , 5.3γ and 5.7γ , in spite of the weaker magnetic response than the electric response in Figure 2. What's more, we note that alone the x axis the distribution pattern of $Re\{\mu_r\}$ shows the evolution of fin-like gradually into spike-like. Then an increasing magnetic response is shown when Δ_p was gradually tuned increasingly. The simultaneously negative permittivity and permeability shown by Figure 2 and Figure 3 prove the 2-D left-handedness in the N-type four-level atomic system.

However, what interested us most is the value and distribution of refractive index in the x-y plane. Figure 4 gives the contour plots for the real part of refractive index $Re\{n\}$ in the x-y plane. The values indicated by the white arrows and distributions of the innermost contour lines corresponding to $Re\{n\}$ attract our intention mostly. Two points are the innermost contour diagram in Figure 4(a), and they get the value being -4.0 for $Re\{n\}$ with their corresponding coordinates $\{0.75\lambda, 0.72\lambda\}$ and $\{0.75\lambda, 0.77\lambda\}$. The innermost contour line changes into one circle with its central coordinate $\{0.75\lambda, 0.75\lambda\}$ in Figure 4(b), and the corresponding value of $Re\{n\}$ is -3.5. When Δ_p is tuned by 5.3 γ and 5.7 γ , the innermost contour lines are still homogeneous and isotropic circles with the same centre coordinate $\{0.75\lambda, 0.75\lambda\}$ in Figure 4(c) and Figure 4(d), respectively. And the values of $Re\{n\}$ corresponding to the innermost contour lines are -3.0, -2.5 in Figure 4(c) and Figure 4(d), respectively. The circle distributions with same

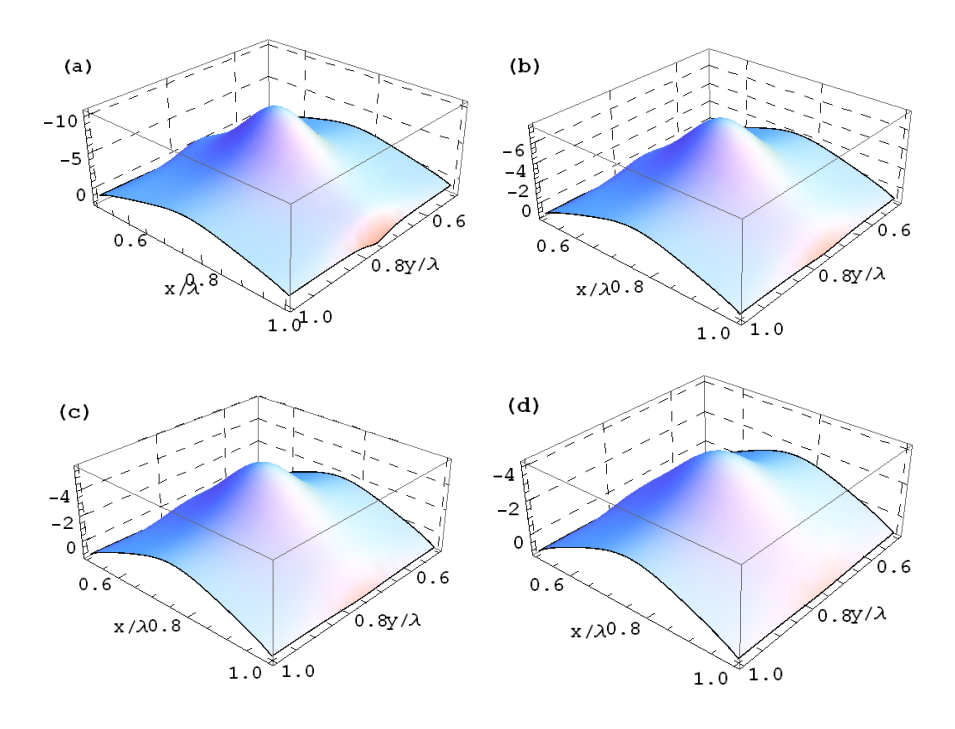


Figure 2: (Color online) Plots for the 2-D $Re\{\varepsilon_r\}$ as a function of (x,y) dependent the probe detuning Δ_p . (a) Δ_p =4.7 γ , (b) Δ_p =5.0 γ , (c) Δ_p =5.3 γ , (d) Δ_p =5.7 γ . The other parameters are Ω_{c0} =10.2 γ , Ω_{s0} =9.5 γ , Δ_c =- Δ_s =-0.15 γ , γ_3 =0.3 γ and γ_4 =0.1 γ , γ =10 8 s⁻¹.

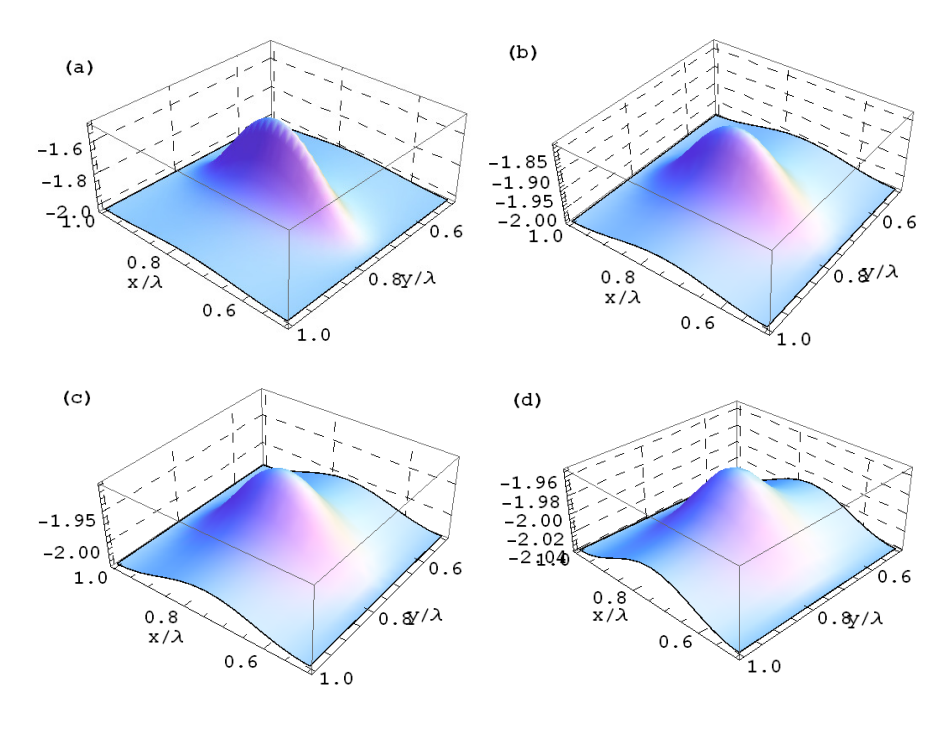


Figure 3: (Color online) Plots for the 2-D $Re\{\mu_r\}$ as a function of (x,y) dependent the probe detuning Δ_p . All the parameters in (a) to (d) are the same as in Figures 2(a) to 2(d), respectively.

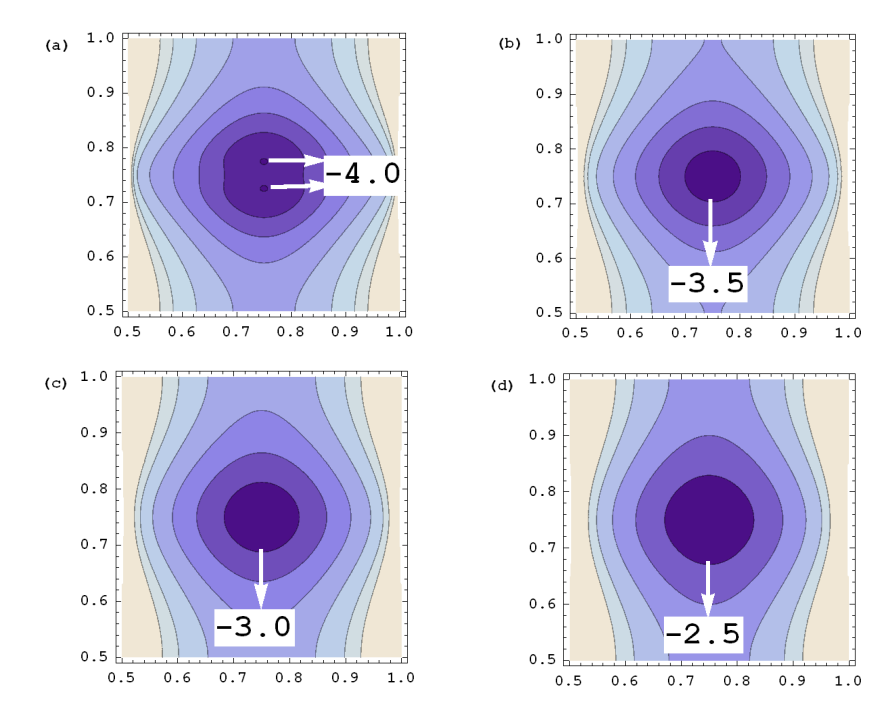


Figure 4: (Color online) Contour plots the 2-D $Re\{n\}$ as a function of (x,y) dependent the probe detuning Δ_p . All the parameters in (a) to (d) are the same as in Figures 2(a) to 2(d), respectively.

centre coordinates in Figure 4(b),(c) and (d) manifest that $Re\{n\}$ can have the same value in all directions. That's to say, $Re\{n\}$ is homogeneous and isotropic in the x-y plane when $Re\{n\}$ gets the following values,-3.5, -3.0, -2.5. The coherent N-type four-level atomic system can be a left-handed media with isotropic NRI when it gets the above mentioned values in the x-y plane.

From the above discussions of Figures 2, 3 and 4, we can see that the real parts of relative permittivity $Re\{\varepsilon_r\}$, permeability $Re\{\mu_r\}$ and refraction index $Re\{n\}$ of the atomic system are sensitive to the probe detuning when the the weak probe light field is placed far of resonance. This is mainly due to the suppression of the spontaneous emission, which is caused by the field-induced interference effect.

4 Conclusion

We suggested a new scenario for 2-D isotropic NRI via two orthogonal standing-wave fields coupling two different atomic transitions in the N-type atomic system. In the x-y plane the simultaneously negative permittivity and permeability exhibit, which means the left-handedness in the N-type atomic system. What's more, $Re\{n\}$ =-3.5, -3.0, -2.5 are both homogeneous and isotropic in the x-y plane

in the same frequency band. Our scheme proposes a new scenario of 2-D isotropic NRI which may give an impetus to some potential advantages or applications. The proposed 2-D isotropic NRI media in our scheme should be paid more attention from both theoretically and experimentally in the near future.

Acknowledgement: Supported by National Natural Science Foundation of China (NSFC) (Grant Nos.61205205 and 6156508508) and the Foundation for talents training projects of Yunnan Province(grant No.KKSY201207068) of China.

References

- J.B. Pendry, A.J. Holden, D.J. Robbins, W.J. Stewart, IEEE Trans. Microwave Theory Tech. 47, 2075 (1999)
- [2] S.A. Schelkunoff, H.T. Friis, Antennas: Theory and Practice (John Wiley and Sons, New York, 1952)
- [3] D.R. Smith, W.J. Padilla, D.C. Vier, S.C. Nemat-Nasser, S. Schultz, Phys. Rev. Lett. 84, 4184 (2000)
- [4] R.A. Shelby, D.R. Smith, S. Schultz, Science 292, 77 (2001)
- [5] V.G. Veselago, Sov. Phys. Usp. 10, 509 (1968)
- [6] E. Cubukcu, Nature 423, 604 (2003)
- [7] A. Grbic, G.V. Eleftheriades, IEEE Trans. Antennas Propag. 51, 2604 (2003)
- [8] R. Mindy, R. Lee, P.M. Fauchet, Opt. Exp. 15, 4530 (2007)

354 — S.-C. Zhao et al. DE GRUYTER OPEN

[9] D. Dorfner, T. Hürlimann, T. Zabel, G. Abstreiter, L.H. Frandsen, J. Finley, Appl. Phys. Lett. 93, 181103 (2008)

- [10] T. Ueda, A. Lai, T. Itoh, IEEE Trans. Microw. Theory Techn. 55, 1280 (2007)
- [11] R. Islam, M. Zedler, G.V. Eleftheriades, IEEE Trans. Antennas Propag. 59, 5 (2011)
- [12] C. Imhof, R. Zengerle, Opt. Express 14, 8257 (2006)
- [13] Z.H. Xiao, K. Kim, Opt. Communs. 283, 2178 (2010)
- [14] Z. Wang, A.X. Chen, Y.F. Bai, W.X. Yang, R.K. Lee, JOSA B 29, 2891 (2012)
- [15] H.R. Hamedi, Arash Radmehr, M. Sahrai, Phys. Rev. A 90,

- 053836 (2014)
- [16] H.R. Hamedi, G. Juzeliūnas, Phys. Rev. A 91, 053823 (2015)
- [17] M.O. Scully, M.S. Zubairy, Quantum Optics (Cambridge Univ. Press, Cambridge, 1997) 7
- [18] J.D. Jackson, Classical Electrodynamics, 3rd Ed (John Wiley Sons, New York, 2001) 4, 159
- [19] D.M. Cook, The Theory of the Electromagnetic Field (Prentice-Hall, Inc., New Jersey, 1975) 11
- [20] J.Q. Shen, J. Almlöf, S. He, Appl. Phys. A 87, 291 (2007)
- [21] M. Ö. Oktel, Ö.E. Müstecaplğlu, Phys. Rev. A 70, 053806 (2004)
- [22] Y.Q. Li, M. Xiao, Opt. Lett. 20, 1489 (1995)